Hindawi
Advances in Civil Engineering
Volume 2019, Article ID 2850916, 15 pages
https://doi.org/10.1155/2019/2850916

Research Article

Analysis of Sluice Foundation Seepage Using Monitoring Data and Numerical Simulation

Fan Xuefeng,[1] Zhenyu Wu ,[2] Liu Lijun,[2] Yanfeng Wen,[3,4] Shu Yu,[3,4] Zhao Zepeng,[2] and Zefa Li[2]

[1]*Kunming Engineering Corporation Limited, Power China, Kunming 650000, China*
[2]*College of Hydraulic and Hydroelectric Engineering, Sichuan University, No. 24 South Section 1, Yihuan Road, Chengdu 610065, China*
[3]*State Key Laboratory of Simulation and Regulation of Water Cycle in River Basin, Beijing 100048, China*
[4]*Department of Geotechnical Engineering, China Institute of Water Resources and Hydropower Research, Beijing 100048, China*

Correspondence should be addressed to Zhenyu Wu; wuzhenyu@scu.edu.cn

Received 3 May 2019; Revised 28 July 2019; Accepted 8 August 2019; Published 19 September 2019

Academic Editor: Eric Lui

For sluices built on soil foundations, seepage safety of the foundation is one of the most concerns during operation of sluices. Monitoring data could reflect the real seepage behavior in the foundation, but of which the shortcoming is that generally only the local seepage states can be measured. The seepage field in the whole foundation can be analyzed by numerical simulation. The permeability coefficients of the foundation materials significantly affect the numerical simulation results; however, it is difficult to accurately determine the values of permeability coefficients. In this paper, an approach based on response surface method (RSM) for calibration of permeability coefficients was proposed, and the efficiency of parameter calibration is improved by constructing the response surface equation instead of time-consuming finite element calculation of foundation seepage. The seepage in a sluice foundation was analyzed using monitoring data and numerical simulation. The monitoring data showed that the seepage pressure in the foundation periodically varies with high value in flood season and low value in dry season. After calibration of the permeability coefficients of the foundation materials using the measured seepage pressure, the seepage fields in the foundation for different water levels were numerically simulated to investigate the cause for the periodical variation of the seepage pressure and the seepage safety of the foundation was assessed with the calculated seepage gradients. The methods adopted in this study could be applied to seepage analysis for sluice foundations with similar geologic conditions and antiseepage measures.

1. Introduction

Sluice is one kind of low-head water retaining structures for purposes of power generation, flood control, irrigation, or water supply. A lot of sluices have been built in mountainous areas of southwest China. The foundations of these sluices are similar in material compositions, seepage characteristics, antiseepage measures, and seepage monitoring. The foundations are generally deep and are composed of modern collapsing deposit layer, solitary gravel layer, sandy loam layer, cobble and gravel layer, floated pebble layer, and so on. Most of the foundations are characterized by strong perviousness and poor seepage stability. Horizontal concrete blanket and vertical concrete cutoff wall (according to the depth of the foundations, closed or suspended cutoff wall is to be used) are generally adopted to control the foundation seepage. The seepage in the sluice foundation is typically monitored with osmometers buried behind the cutoff wall.

The monitoring data of seepage pressure can reflect the real seepage behavior in sluice foundation, whereas the shortcomings are that just local seepage states could be observed due to limited measuring points. The seepage field in the whole concerned area can be analyzed using numerical simulation techniques, such as finite element method (FEM), and the effects of material composition, seepage characteristics of various materials, seepage control

measures, and seepage boundary conditions on the seepage field can be investigated. Therefore, numerical simulation has been extensively applied to seepage analysis of foundation seepage (e.g., [1–8]). The values of seepage parameters such as permeability coefficients have a great influence on the numerical simulation results of foundation seepage. If the parameter values for computation are wrongly determined, the seepage calculation results may considerably deviate from the real situations and the seepage safety may be misjudged. Seepage parameters could be calibrated with seepage monitoring data, and numerical simulation using the calibrated parameters would yield more realistic results. Typical calibration methods for geotechnical parameters include simulated annealing technique [9, 10], particle swarm optimization [11–13], neural network and genetic algorithm [14–17], Nelder–Mead algorithm [13, 18], response surface method (RSM) [19–21], and support vector machine [22].

A sluice is located on the main stream of Minjiang River in Sichuan Province, China. Its main function is to generate electricity. The sluice has experienced the Wenchuan earthquake. Since the dam site is close to the epicenter, the sluice was seriously damaged. After the earthquake, the sluice was repaired and restored impounding by the end of 2009. The foundation of the sluice is mainly composed of floated pebble layers and sand layers. Seepage safety of the foundation is one of the most concerns after the recovery of the sluice. Eight osmometers were embedded in the borehole behind the cutoff wall to monitor the variation of seepage pressure in the sluice foundation. Based on the monitoring data during the period from 2010 to 2016, the variation of seepage pressure in the sluice foundation and its causes were firstly investigated. Then, the permeability coefficients of the foundation materials were calibrated using a RSM-based method with the seepage pressure monitoring data. Finally, the seepage fields within the sluice foundation in dry season and flood season were, respectively, analyzed using FEM to interpret the variation of seepage pressure, and the seepage safety of the sluice foundation was assessed with the computed seepage gradients in the foundation.

2. Analysis of Monitoring Data of Seepage Pressure in a Sluice Foundation

2.1. Brief Introduction for the Sluice. The sluice is located on the main stream of the Minjiang River in Sichuan Province, China. It was built in 1970s. The total storage capacity of the reservoir is 930,000 m^3, the normal water level is 945.00 m, the design flood level is 945.60 m, and the maximum flood level is 948.87 m. The main function of the sluice is to generate electricity. On May 12, 2008, an earthquake with the Richter scale of 8.0 occurred in Wenchuan, Sichuan Province, China. The sluice is close to the epicenter and was severely damaged during the earthquake. After the earthquake, the sluice was repaired and the power generation was recovered by the end of 2009. Seepage safety of the foundation is one of the most concerns for the sluice.

The sluice mainly consists of floodgates, sand sluicing gates, non-overflow dam, water intake, and trash rack. The length of the sluice is 156 m and 25 m in transverse direction and stream direction, respectively. The maximum height of the sluice is 21.4 m. The maximum depth of the foundation is 45 m, and the upstream concrete blanket and suspended cutoff wall are adopted to control seepage. The cutoff wall is located on the upstream side and is 20 m distant from the sluice chamber. The cutoff wall is 0.7 m thick and has a maximum depth of 27 m. The length of the upstream blanket ranges between 75 m and 95 m, and the length of the downstream apron is 56 m. The bank slopes on both sides of the river are gently inclined at the sluice site, and the slope height ranges from 300 m to 500 m. The width of the riverbed is between 80 m and 100 m. The sluice foundation is mainly composed of floated pebble layer and sandy loam layer, and the thicknesses of which approximately ranges from 40 m to 62 m. The longitudinal section and cross section of the sluice and its foundation are shown in Figures 1–3.

In order to monitor the seepage pressure in the sluice foundation and the antiseepage effect of the upstream blanket and suspended cutoff wall, eight osmometers were installed in two rows on the downstream side of the cutoff wall paralleled to the sluice axis, among which five osmometers (UP1~UP5) are arranged in the upstream row and three osmometers (UP6~UP8) are laid in the downstream row. Figure 4 shows the seepage monitoring layout for the sluice foundation.

2.2. Analysis of the Monitoring Data of Seepage Pressure in the Sluice Foundation. The seepage pressure in the sluice foundation is analyzed with the monitoring data from January 2010 to December 2016. In order to compare with the reservoir water level, the measured original values of seepage pressure have been transformed into water level elevations in terms of the seepage pressure head and the installation elevation of the osmometers. Osmometers UP3 and UP6 had not recorded monitoring data from January 2010 to December 2012 due to malfunction. The time series of the seepage pressure and reservoir water level are shown in Figures 5–12. From 2010 to 2016, the reservoir water level generally varied between 943.50 m and 945.00 m. The highest water level was 945.49 m, which occurred on June 5, 2013. The lowest water level was 939.50 m, which happened on January 6, 2011 (emptying of the reservoir for inspection).

It can be seen from Figures 5–12 that the measured values show an obvious periodical variation of the seepage pressure, that is, the seepage pressure is relatively high in flood season (from May to October) and is relatively low in dry season (from November to April). The measured maximum value of seepage pressure for each osmometer occurred in July is between 938.34 m and 945.15 m (due to the impact from the debris flow on July 9, 2013, the downstream water level is higher than 945 m and the corresponding values of seepage pressure for most osmometers are highest). The measured minimum value occurred in

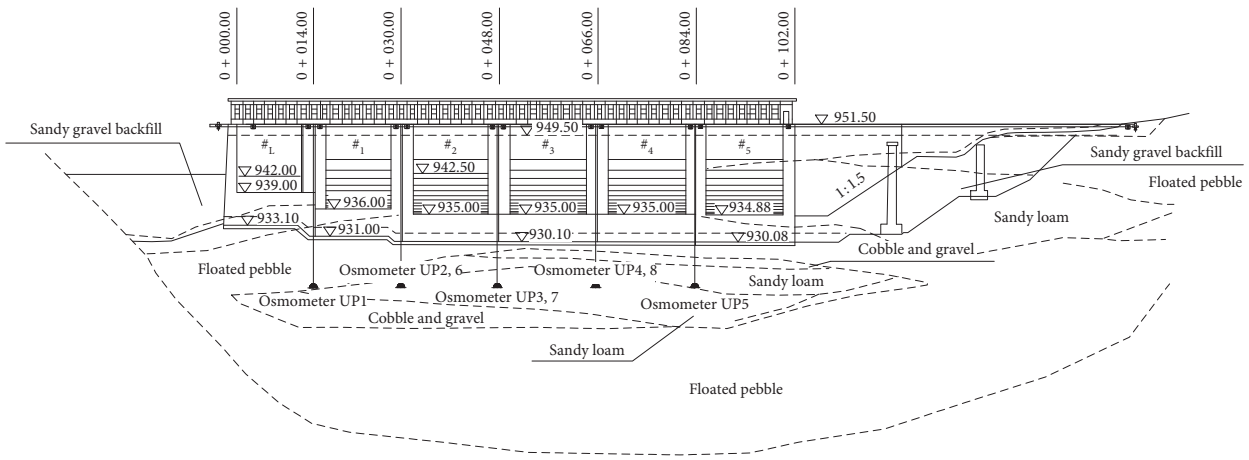

Figure 1: Longitudinal section for sluice foundation.

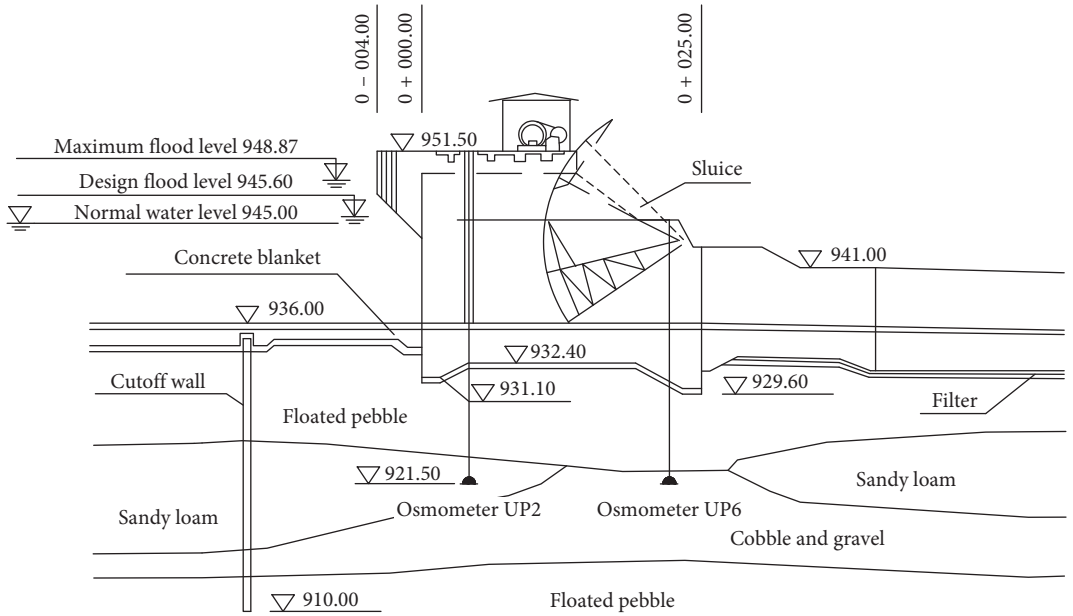

Figure 2: Cross section for 1# sluice foundation.

December and April is between 935.07 m and 939.34 m. Statistical analysis of the measured values of seepage pressure for all osmometers from 2010 to 2016 shows that the amplitudes of annual fluctuation of measured values are between 2.08 m and 8.89 m, while the corresponding amplitudes of annual fluctuation of reservoir water level are smaller than 2.75 m, and 65% of which are less than 1 m and only a few exceed 2 m. It is indicated that the correlation between the measured seepage pressure and reservoir water level is weak, and the variation of reservoir water level may not be the main reason for the periodical fluctuation of the seepage pressure.

In dry season, the floodgates and sand sluicing gates are closed. There is essentially no water in the downstream riverbed next to the sluice, as the water is transmitted from the water intake to the distant power plant. In flood season, the gates are opened and the downstream river water level is high. According to the layout of antiseepage measures (the upstream concrete blanket and the suspended cutoff wall which is located on the upstream side of the sluice chamber) for the foundation, as shown in Figures 2 and 3, their main purpose is to minimize the seepage from the upstream reservoir to downstream river. As the antiseepage measures could not prevent the water in the downstream river entering into the foundation, the periodical variation of seepage pressure in the foundation may be caused by the fluctuation of water level in the downstream river in dry and flood seasons.

Since there are no monitoring data for the downstream water level, the relationship between the measured seepage pressure and the downstream water level cannot be quantitatively investigated by monitoring data analysis and will be analyzed using numerical simulation. In addition, the number of osmometers is limited and just local seepage around the osmometers can be observed; thus, the overall seepage states within the sluice foundation cannot be

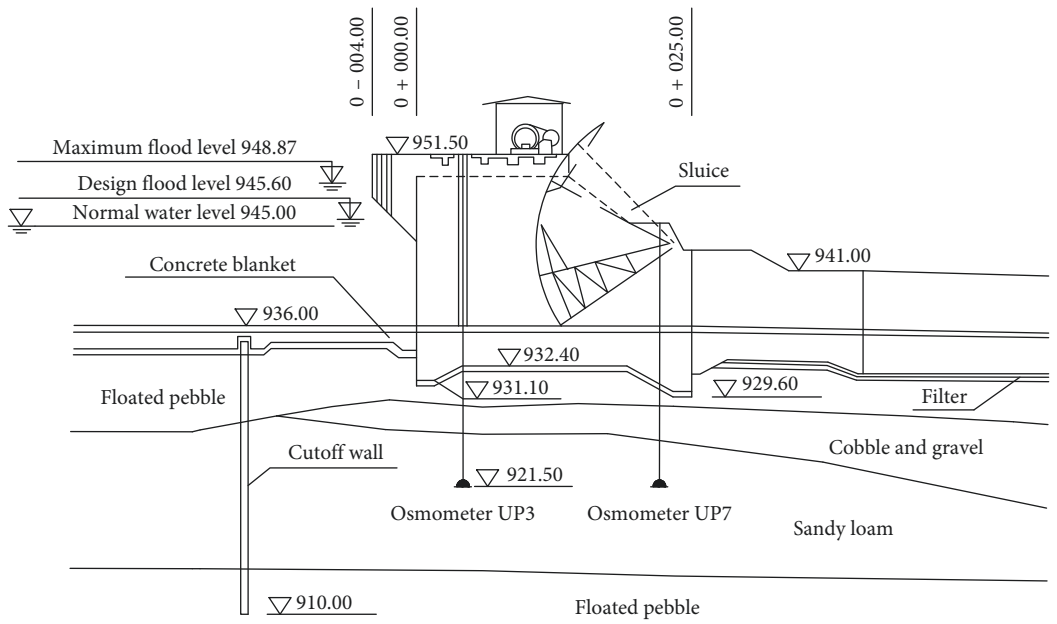

Figure 3: Cross section for 2# sluice foundation.

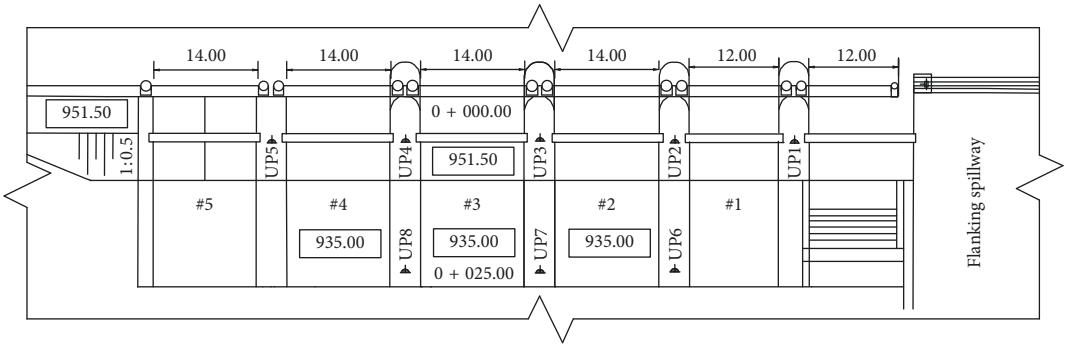

Figure 4: Seepage monitoring layout for sluice foundation.

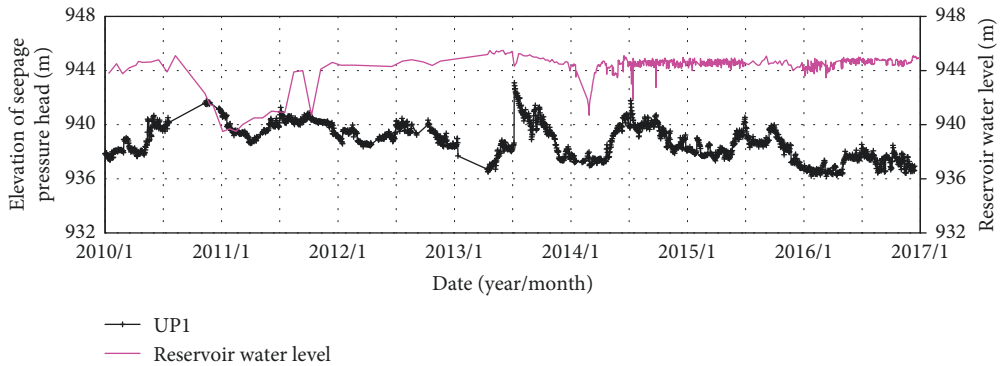

Figure 5: Time series for seepage pressure head at UP1 and reservoir water level.

evaluated. In the following sections, FEM is adopted to simulate the seepage field in the foundation and to assess seepage safety. In order to make the simulation results more close to the actual situation, the permeability coefficients of the foundation materials are calibrated first based on the monitoring data of seepage pressure.

3. Calibration of the Permeability Coefficients for the Foundation Materials

3.1. Finite Element Model. Commercial FEM software ANSYS [23] is applied to establish the 2D finite element models of the 1# and 2# sluice foundation sections. The FEM

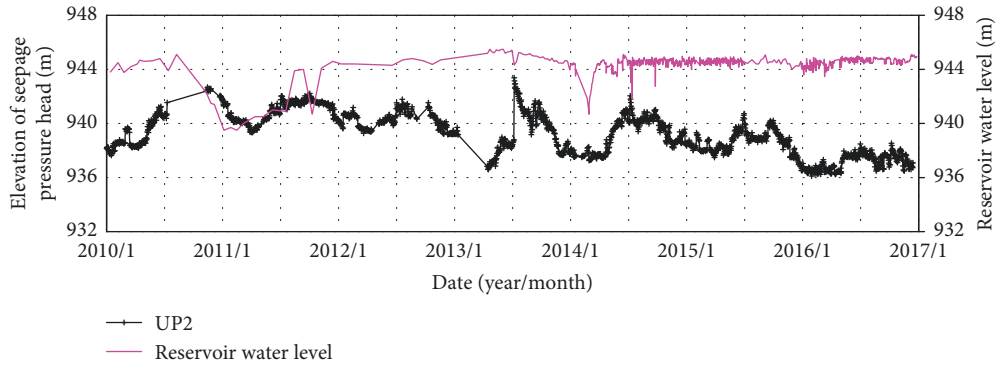

Figure 6: Time series for seepage pressure head at UP2 and reservoir water level.

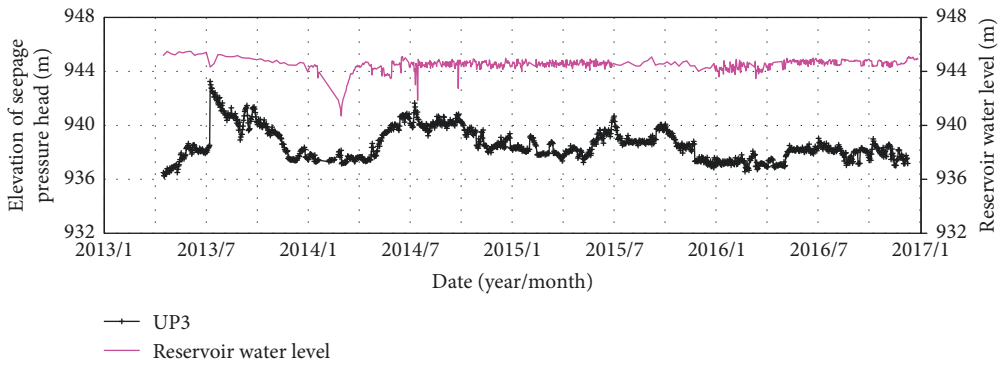

Figure 7: Time series for seepage pressure head at UP3 and reservoir water level.

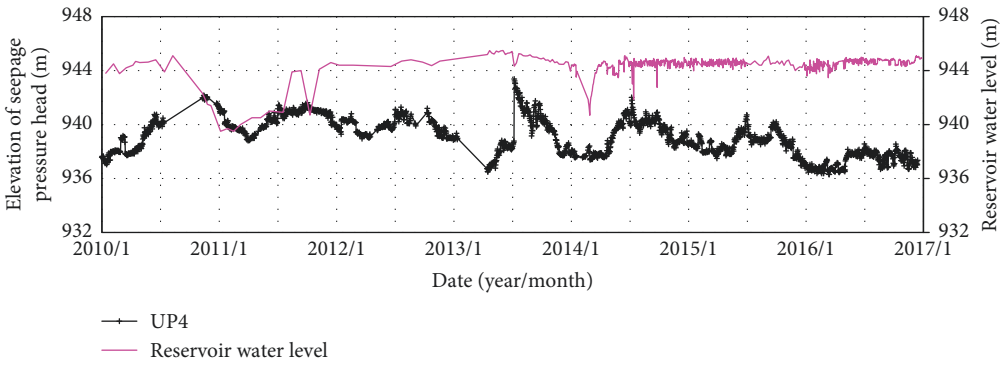

Figure 8: Time series for seepage pressure head at UP4 and reservoir water level.

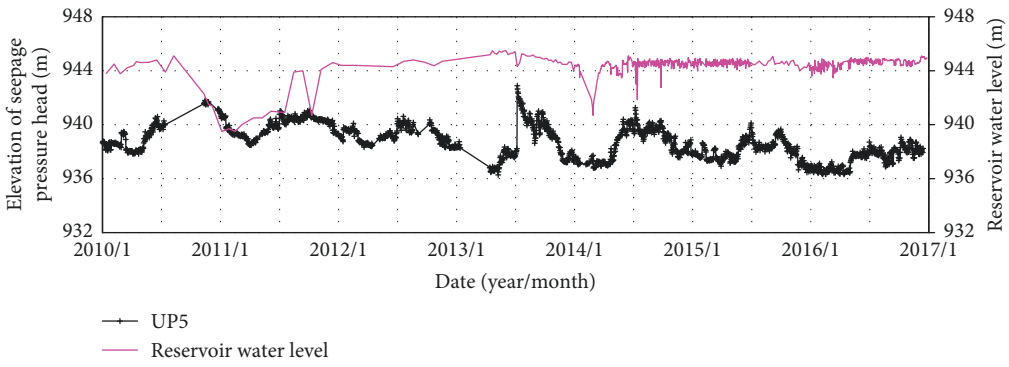

Figure 9: Time series for seepage pressure head at UP5 and reservoir water level.

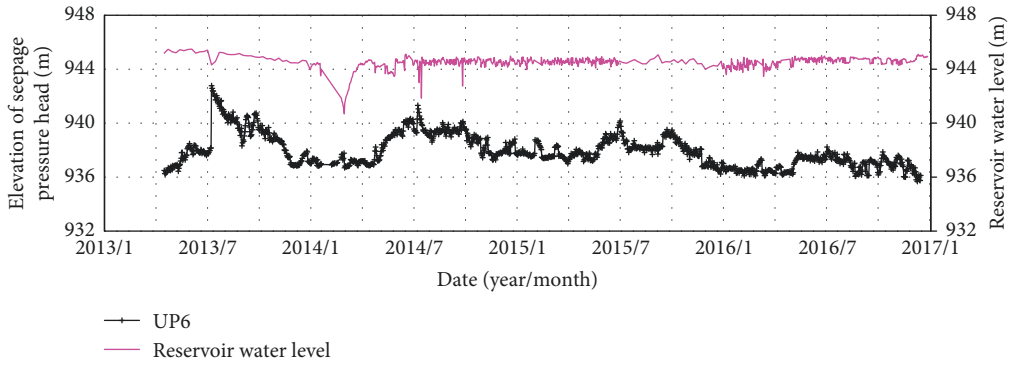

Figure 10: Time series for seepage pressure head at UP6 and reservoir water level.

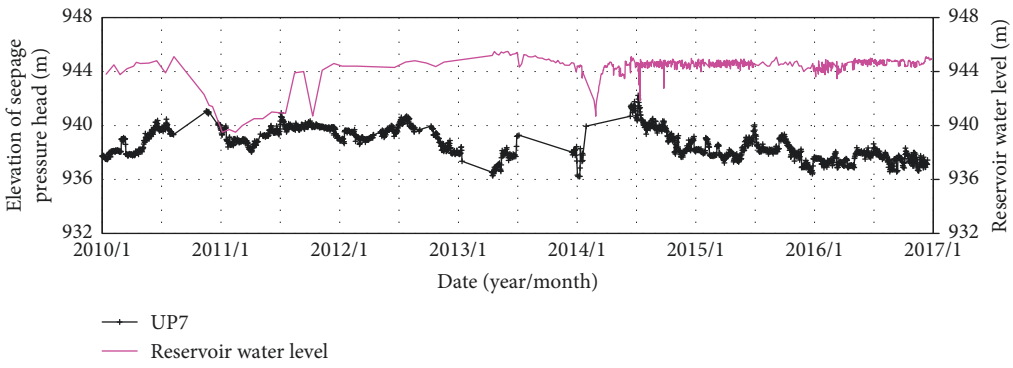

Figure 11: Time series for seepage pressure head at UP7 and reservoir water level.

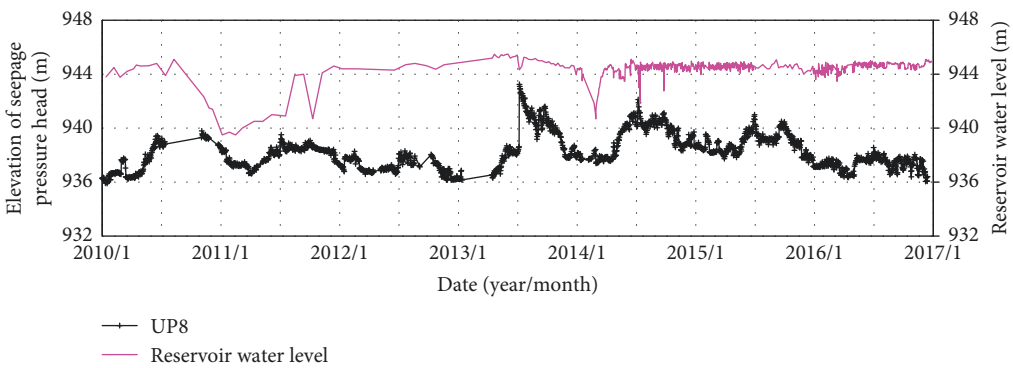

Figure 12: Time series for seepage pressure head at UP8 and reservoir water level.

consists of sluice floor slab, upstream blanket, downstream apron (including drainage holes), cutoff wall, soil layers, and granite rock bed, as shown in Figures 13 and 14. The drainage holes in the apron are simulated by increasing the permeability coefficient of the elements at the corresponding position. The FEM extends 75 m upstream from the upstream edge of the blanket, 80 m downstream from the downstream edge of the apron, and 50.4 m downward from the bottom of the soil foundation. In order to compare the calculated and measured seepage pressures, monitoring nodes in the finite element model are fixed at positions where the osmometers are located. The osmometers UP2, UP6 and UP3, UP7 are buried in the foundations of the 1# and 2# sluice chambers, respectively.

Because the basic equations of seepage analysis and thermal analysis are similar [24], the thermal analysis module of ANSYS software is utilized to simulate the seepage field in the sluice foundation. The finite element models are discretized using plane thermal element PLANE55. The finite element models for the 1# and 2# sluice foundation sections are discretized into 6922 elements and 7095 nodes and 6354 elements and 6527 nodes, respectively. The lateral and bottom boundaries of the models are assumed as impervious boundaries. The nodes on the top boundary of the models are assigned fixed water heads in terms of the corresponding reservoir and downstream water levels in dry and flood seasons. There are monitoring data for reservoir water level; however, no data are available for

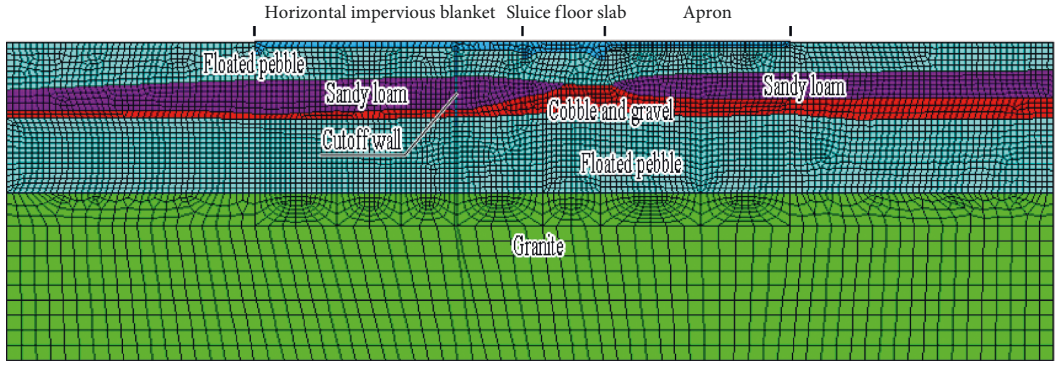

Figure 13: Finite element mesh for 1# sluice foundation.

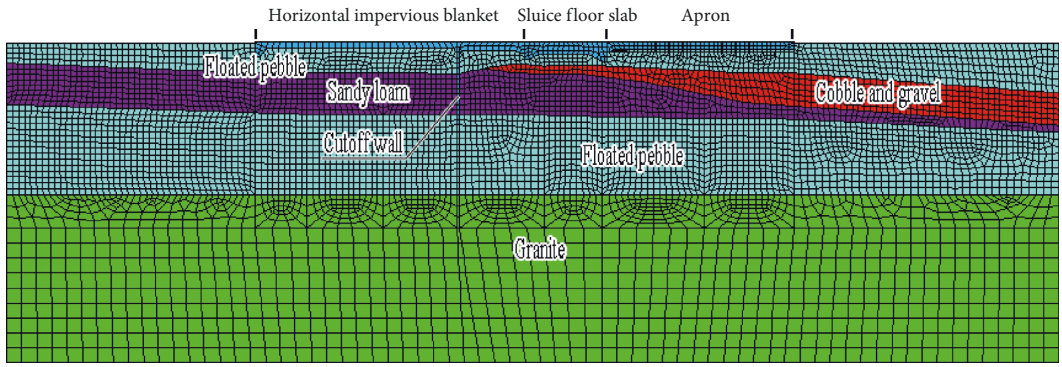

Figure 14: Finite element mesh for 2# sluice foundation.

downstream water level. In this study, it is assumed that there is no water in the downstream river in dry season (as the water is transmitted from the water intake to the distant power plant). In flood season, all gates are opened. Therefore, the downstream water level can be calculated by hydraulic calculation based on parameters such as flood discharge, gate size, and river section.

3.2. Calibration Method for Permeability Coefficients. There are experimental values of permeability coefficients for concrete (the construction material for sluice floor slab, blanket, apron, and cutoff wall) and granite. However, due to the difficulties in extracting in situ samples and performing laboratory test on samples containing large particles, the values of permeability coefficients for the foundation materials are estimated by geological survey and engineering judgment and are of considerable uncertainty. Therefore, it is necessary to calibrate the permeability coefficients based on the monitoring data of seepage pressure.

Calibration of the permeability coefficients means finding such values of permeability coefficients that the computed seepage pressures are most close to the measured ones; thus, it is needed to solve an optimization problem in which the objective function is established using the computed and measured values of seepage pressure, and the computed seepage pressure is a function of the permeability coefficients. In the process of solving the optimization problem, a large number of computations of the seepage pressure with different values of permeability coefficients are required. As the seepage pressure is computed using FEM, the calibration process is time-consuming. In order to improve the calibration efficiency, response surface equations are utilized instead of FEM to compute seepage pressure.

In this study, the following quadratic polynomial response surface equation [25, 26] is adopted:

$$H(\overline{K}) = C + \sum_{i=1}^{n} a_i K_i + \sum_{i=1}^{n-1} \sum_{j=i+1}^{n} b_{ij} K_i K_j + \sum_{i=1}^{n} c_i K_i^2, \quad (1)$$

where $H(\overline{K})$ is the calculated value of seepage pressure, which is a function of the permeability coefficients $\overline{K} = (K_1, K_2, \ldots, K_n)$; K_i and K_j are the permeability coefficients of ith and jth material; a_i, b_{ij}, c_i, and C are coefficients to be determined; and n is the number of foundation materials whose permeability coefficients need to be calibrated.

Seepage field in the foundation is computed using FEM with different combinations of values of the permeability coefficients to be calibrated. Then, the coefficients in equation (1) can be obtained by regression analysis with the calculated seepage pressures at the monitoring nodes and the corresponding measured seepage pressures. The orthogonal design [27, 28] is adopted to produce the combinations of values of the permeability coefficients for seepage computation. The orthogonal design for three materials is illustrated in Figure 15. As shown in Figure 15, the combination

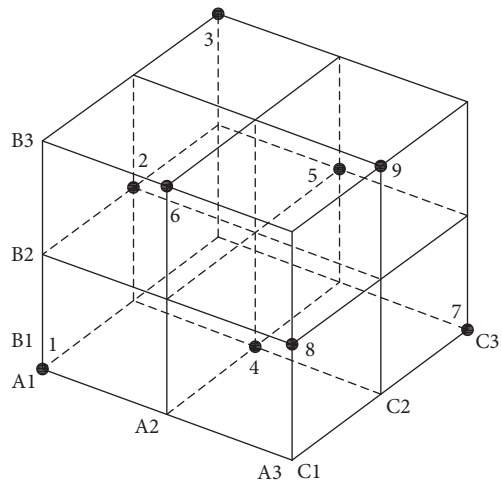

Figure 15: Diagrammatic sketch for orthogonal design. The black dots are the combinations of values of the permeability coefficients for materials A, B, and C Three values of permeability coefficient for each material are considered.

scheme obtained by the orthogonal design is random, and all the test points in the scheme are uniformly dispersed, which can well represent the situation of a large number of test points.

With equation (1) and the measured values of seepage pressure, the objective function for calibration of permeability coefficients can be established as follows:

$$\text{Min}\left[F\left(\overline{K}\right)\right] = \text{Min}\left\{\sum_{k=1}^{m}\sum_{i=1}^{l}\left[H_i^k\left(\overline{K}\right) - \widehat{H}_i^k\right]^2\right\}, \tag{2}$$

$$K_j^{\min} \le K_j \le K_j^{\max}, \quad j = 1, 2, \ldots, n, \tag{3}$$

where $F(\overline{K})$ is the objective function, which is a function of the permeability coefficients $\overline{K} = (K_1, K_2, \ldots, K_n)$; $H_i^k(\overline{K})$ is the response surface equation for calculating the seepage pressure at ith monitoring node under kth operational condition and $\widehat{H}_i^k$ is the corresponding measured value of seepage pressure; $K_j^{\min}$ and $K_j^{\max}$ are the upper and lower limits of the permeability coefficient of jth material, respectively; m is the number of operational conditions; n is the number of materials whose permeability coefficients need to be calibrated; and l is the number of monitoring nodes.

The calibration process for the permeability coefficients is to search for a group of values of the permeability coefficients in the specified ranges so that the objective function is minimized. Therefore, the calibration process is actually a nonlinear programming problem with constraint conditions. The software LINGO [29] is applied to solve the nonlinear programming problem expressed by equations (2) and (3). Figure 16 shows the procedure for calibration of permeability coefficients.

3.3. Results of the Calibration for Permeability Coefficients of the Foundation Materials. According to the monitoring data of seepage pressure from four osmometers (UP2, UP3, UP6, and UP7) in flood and dry seasons of 2015, the permeability coefficients of floated pebble, cobble and gravel, and sandy loam layers are calibrated using the method described in the preceding section. There are three permeability coefficients to be calibrated; hence, the response surface equations as equation (1) have 10 coefficients to be determined. In order to produce enough combinations of values of the permeability coefficients for regression analysis, five values μ, $\mu(1-\delta)$, $\mu(1+\delta)$, $\mu(1-3\delta)$, and $\mu(1+3\delta)$ of the permeability coefficient for each material are considered in the orthogonal design, where μ and δ are design value (listed in Table 1) and coefficient of variation of the permeability coefficient. According to [30], δ is assumed to be 0.3. The orthogonal design module of SPSS software [31] is utilized to obtain the combinations of values of the permeability coefficients. Specific combinations are shown in the orthogonal design table, as shown in Table 2. Then, the seepage pressures in the foundation are computed using the finite element models shown in Figures 13 and 14 with different combinations of permeability coefficients. The regression analysis module of SPSS software is adopted to obtain the coefficients of eight response surface equations for the seepage pressures at four monitoring nodes corresponding to the measuring points UP2, UP3, UP6, and UP7 in flood and dry seasons, respectively. The multiple correlation coefficients of the regression analysis for the eight response surface equations are all greater than 0.9. Moreover, the differences between the seepage pressures calculated using the response surface equations and FEM are quite small, and the maximum relative error is less than 0.34%. Therefore, the response surface equations could be utilized instead of FEM to compute seepage pressure in the calibration process.

The objective function as equation (2) is established using the response surface equations and the measured values of seepage pressure from the osmometers UP2, UP3, UP6, and UP7. The upper and lower limits of the permeability coefficient are specified as $\mu(1+3\delta)$ and $\mu(1-3\delta)$, respectively. The LINGO software is applied to search for the

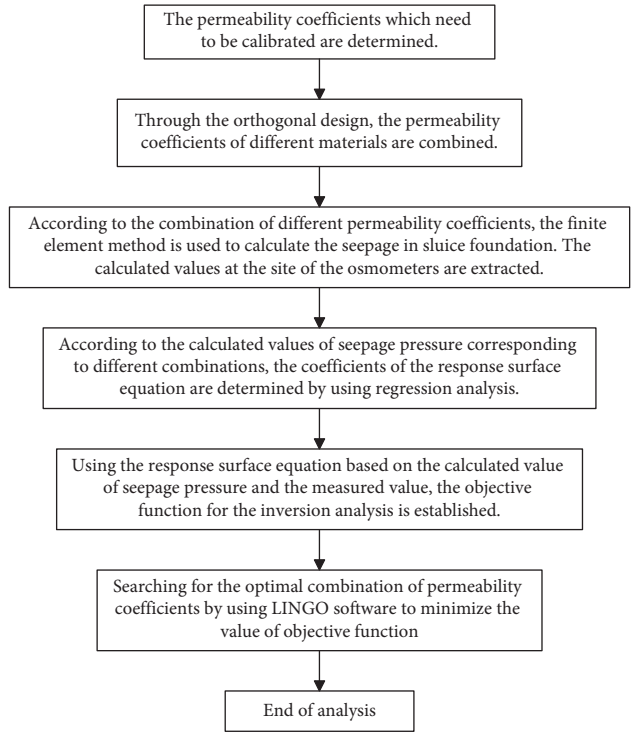

Figure 16: Flowchart for calibration of permeability coefficients.

Table 1: Design value and calibrated value of permeability coefficients.

Material	Design value K (m/s)	Calibrated value K' (m/s)
Floated pebble	8.12×10^{-5}	6.85×10^{-5}
Cobble and gravel	4.64×10^{-5}	5.49×10^{-5}
Sandy loam	2.31×10^{-5}	8.24×10^{-6}
Cutoff wall	1.00×10^{-9}	—
Horizontal impervious blanket, sluice floor slab, and apron	1.00×10^{-9}	—
Granite	1.00×10^{-7}	—

optimal combination of values of the permeability coefficients for the floated pebble, cobble and gravel, and sandy loam layers to minimize the objective function. The calibration results are shown in Table 1. It can be seen from Table 1 that there is a large difference between the calibrated value and design value of the permeability coefficient for sandy loam. The seepage pressure in the sluice foundation is computed using the calibrated values of the permeability coefficients. Figures 17 and 18 show the comparison between calculated and measured seepage pressures at the measuring points UP2, UP3, UP6, and UP7. It can be seen that the calculated seepage pressures overall agree with the measured ones. The differences between calculated and measured seepage pressures may be due to the measurement error of the osmometers and the simulation error of the finite element model (a three-dimensional model is better; additionally, the geologic conditions of the foundation for establishing the finite element model are inferred based on limited boreholes and may differ from the actual situation).

4. Seepage Analysis of the Sluice Foundation Using FEM

4.1. Investigation on the Cause of the Variation of Seepage Pressure in the Foundation. According to the analysis of monitoring data, the primary cause of the periodical variation of the seepage pressures measured by the osmometers may be the large fluctuation of water level in the downstream river during flood and dry seasons. In this section, the cause of the variation of seepage pressure in the foundation is investigated through comparison of the effects of reservoir and downstream water level on seepage pressures. In order to investigate the effect of reservoir water level, the downstream water level is fixed at 936 m, whereas the reservoir water level is increased from 942.5 m to 945 m with an increment of 0.5 m, and the corresponding seepage pressures at the measuring points UP2, UP3, UP6, and UP7 are computed using FEM. In turn, the reservoir water level is fixed at 944.5 m, while the downstream water level is raised from 936 m to 938.5 m with an increment of 0.5 m, and the corresponding seepage pressures are computed to investigate the effect of downstream water level. As shown in Figure 19, the seepage pressures at the measuring points increase linearly with the rise of the reservoir or downstream water level. The increase rate of seepage pressure with the rise of downstream water level is obviously larger than that with the rise of reservoir water level. The increase in seepage pressure is less than 1 m when the reservoir water level is raised by 2.5 m; in contrast, the increase in seepage pressure is between 2 m and 2.5 m when the downstream water level is raised by 2.5 m. Therefore, the variation of

Table 2: Orthogonal design table of permeability coefficients.

Experimental number	First orthogonal design			Second orthogonal design		
	k_1 (m/s)	k_2 (m/s)	k_3 (m/s)	k_1 (m/s)	k_2 (m/s)	k_3 (m/s)
1	$1.06E-04$	$3.00E-05$	$3.25E-05$	$8.12E-05$	$2.31E-06$	$4.64E-05$
2	$5.68E-05$	$2.31E-05$	$6.03E-05$	$1.54E-04$	$2.31E-06$	$8.82E-05$
3	$1.06E-04$	$1.62E-05$	$6.03E-05$	$8.12E-06$	$4.39E-05$	$4.64E-05$
4	$5.68E-05$	$3.00E-05$	$4.64E-05$	$8.12E-05$	$4.39E-05$	$8.82E-05$
5	$8.12E-05$	$3.00E-05$	$6.03E-05$	$8.12E-06$	$2.31E-06$	$4.64E-06$
6	$1.06E-04$	$2.31E-05$	$4.64E-05$	$8.12E-05$	$2.31E-05$	$4.64E-06$
7	$8.12E-05$	$2.31E-05$	$3.25E-05$	$8.12E-06$	$2.31E-05$	$8.82E-05$
8	$8.12E-05$	$1.62E-05$	$4.64E-05$	$1.54E-04$	$4.39E-05$	$4.64E-06$
9	$5.68E-05$	$1.62E-05$	$3.25E-05$	$1.54E-04$	$2.31E-05$	$4.64E-05$

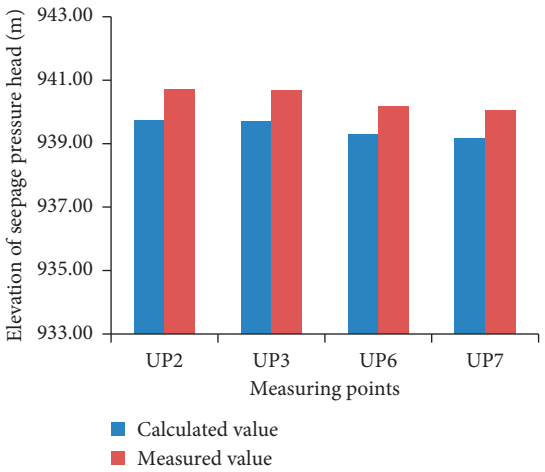

Figure 17: Comparison of calculated value and measured value in flood season.

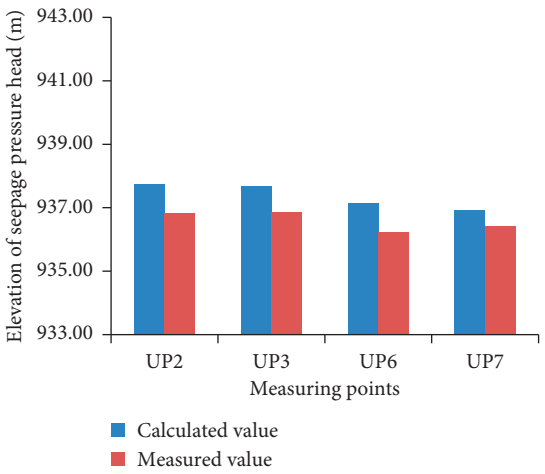

Figure 18: Comparison of calculated value and measured value in dry season.

seepage pressure in the sluice foundation is mainly affected by the downstream water level.

4.2. Characteristics of Seepage in the Sluice Foundation. The seepage fields in flood season (the reservoir water level is 944.60 m, and the downstream water level is 938.50 m) and dry season (the reservoir water level is 944.59 m, and the downstream water level is 936.00 m) are simulated using FEM with the calibrated permeability coefficients of foundation materials. The total seepage head contours in the foundation are shown in Figures 20–23. It can be seen that the total seepage head in the foundation decreases from upstream to downstream and rapidly drops from the upstream side to downstream side of the cutoff wall, which indicates that the cutoff wall plays an important role in

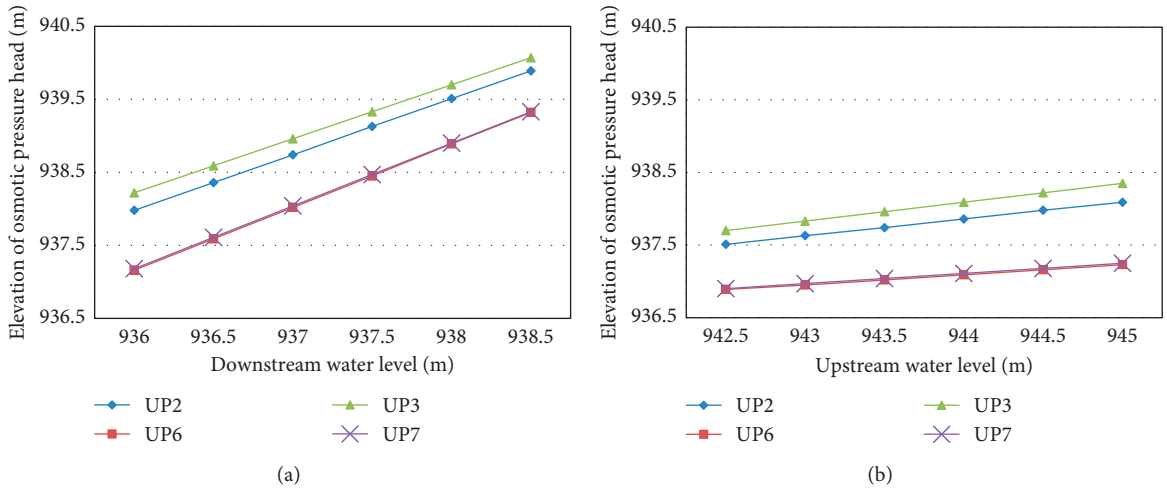

Figure 19: (a) Effects of downstream water level on seepage pressure at the measuring points UP2, UP3, UP6, and UP7. (b) Effects of reservoir water level on seepage pressure at the measuring points UP2, UP3, UP6, and UP7.

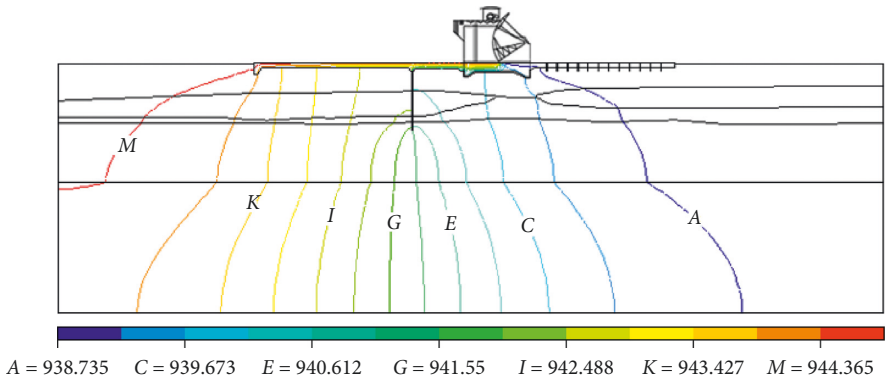

Figure 20: Total seepage head contour in 1# sluice foundation in flood season.

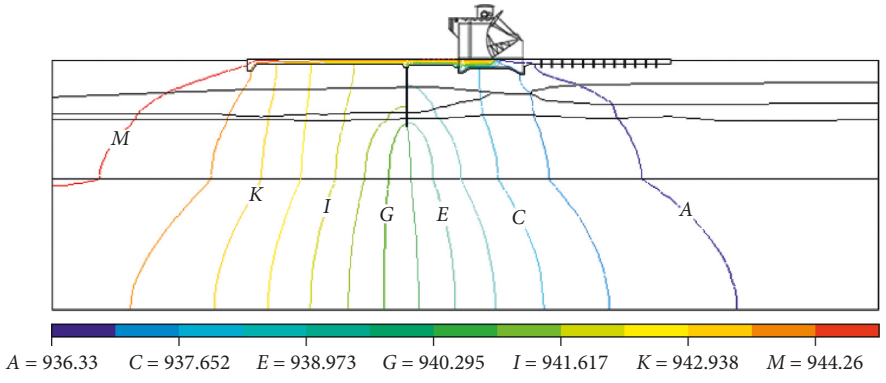

Figure 21: Total seepage head contour in 1# sluice foundation in dry season.

reducing the seepage pressure in the sluice foundation. Since the cutoff wall cannot prevent the downstream river water from flowing into the foundation in flood season, the seepage pressure behind the cutoff wall is obviously larger than that in dry season.

The seepage gradients in the foundation are shown in Figures 24–27. It can be observed that the seepage gradients around the base of the cutoff wall are the largest, and the seepage gradients are rather large near the upstream edge of the concrete blanket and the drainage holes in the upstream part of the apron. However, the seepage gradients in most regions of the foundation are quite small; thus, the seepage in the foundation is essentially stable. Due to the large difference between upstream and downstream water levels in dry season, the seepage gradients in the foundation are larger than those in flood season. The maximum seepage gradients

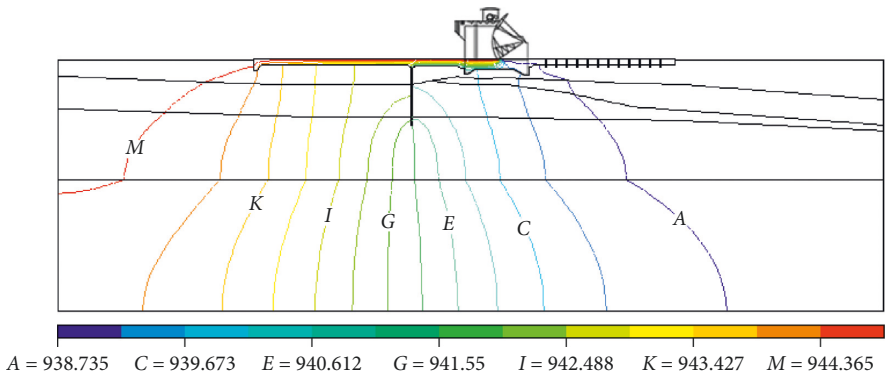

Figure 22: Total seepage head contour in 2# sluice foundation in flood season.

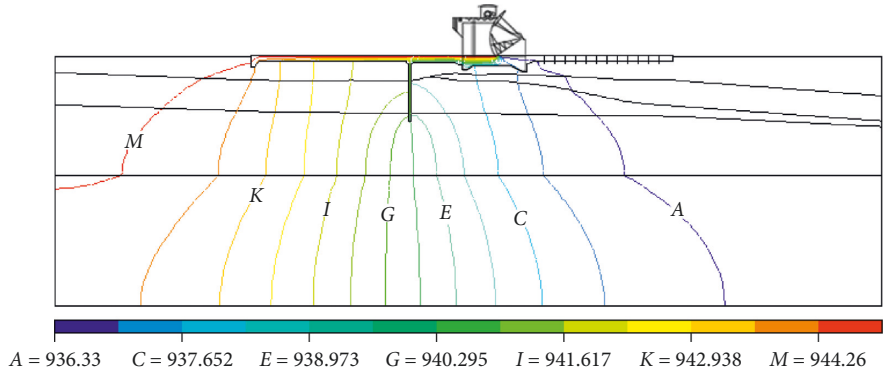

Figure 23: Total seepage head contour in 2# sluice foundation in dry season.

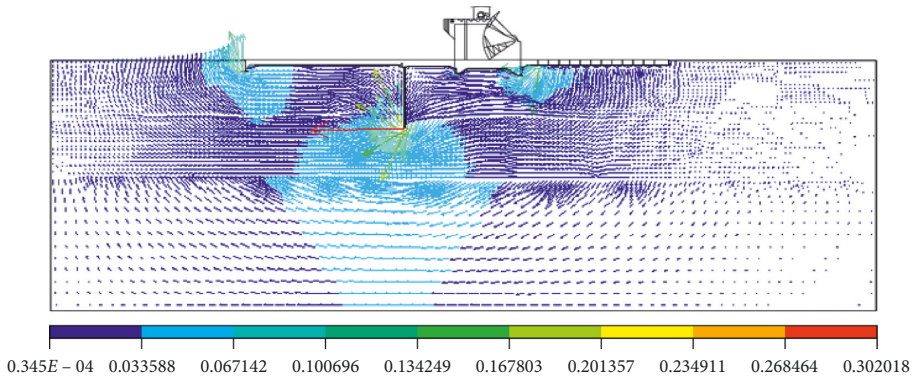

Figure 24: Seepage gradients in 1# sluice foundation in flood season.

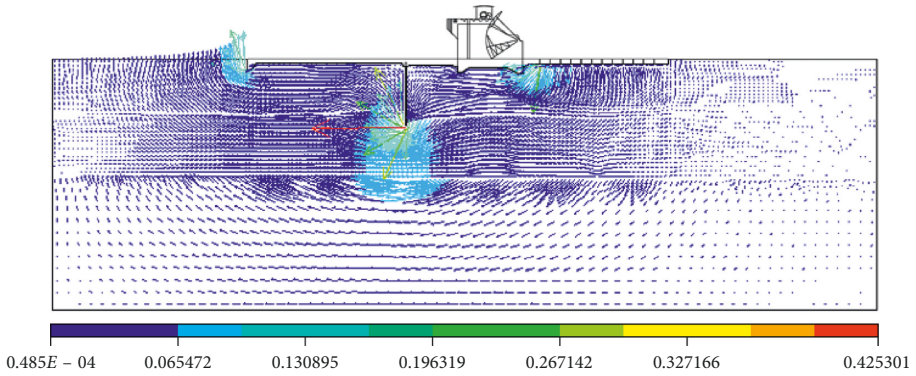

Figure 25: Seepage gradients in 1# sluice foundation in dry season.

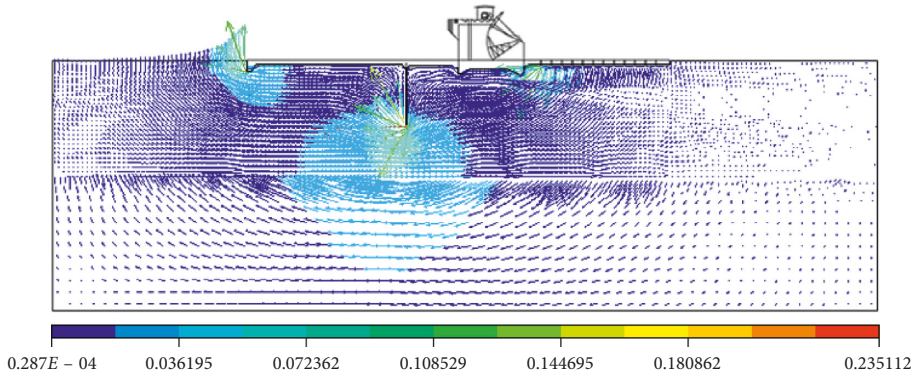

Figure 26: Seepage gradients in 2# sluice foundation in flood season.

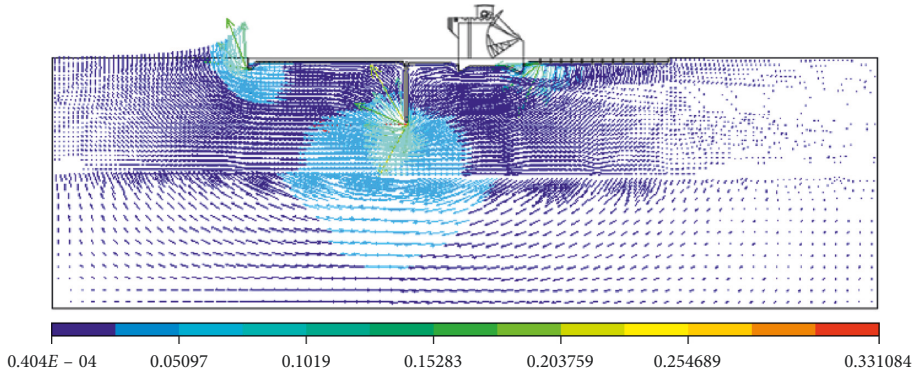

Figure 27: Seepage gradients in 2# sluice foundation in dry season.

near the base of the cutoff wall, the upstream edge of the concrete blanket, and the drainage holes in the apron are 0.302, 0.129, and 0.148 in flood season and are 0.425, 0.181, and 0.209 in dry season, respectively. Simulation results indicate that there are relatively high risks of seepage failure near the base of the cutoff wall, the upstream edge of the concrete blanket, and the drainage holes in the apron. As there is no seepage monitoring equipment in those risky regions, visual inspection should be performed, especially in dry season, to monitor whether abnormal seepage phenomenon occurs such as vortices in the reservoir in front of the sluice or large flow with fine soil particles in the drainage hole of the apron. Until now, there is no abnormal seepage phenomenon observed.

5. Summary and Conclusions

(1) Seepage monitoring for sluice foundation is typically implemented using osmometers installed behind the cutoff wall. Although seepage monitoring could reflect realistic seepage state in the sluice foundation, its drawbacks are that measuring points are limited and just local seepage state could be observed. Seepage in the whole foundation can be analyzed using numerical simulation such as FEM. However, permeability coefficients of foundation materials which significantly affect seepage simulation are commonly estimated by geological survey and engineering judgment and are of considerable uncertainty. Therefore, calibration of material permeability coefficient should be carried out before numerical simulation.

(2) In this paper, a RSM-based calibration method for permeability coefficients is proposed.The efficiency of the calibration process is improved by response surface equations instead of time-consuming FEM for computation of seepage pressure.

(3) As a case study, the seepage in a sluice foundation was analyzed using monitoring data and numerical simulation. Analysis of monitoring data and numerical simulation results indicates that the variation of the seepage pressure is primarily caused by the fluctuation of downstream water level during flood and dry seasons.

(4) The seepage fields in the foundation in dry and flood seasons were simulated using FEM with the calibrated permeability coefficients. The simulation results indicate that the cutoff wall plays an important role in reducing seepage pressure of the foundation and the seepage pressure in flood season is larger than that in dry season. The seepage gradients in most regions of the foundation are quite small and are rather large near the base of the cutoff wall, the upstream edge of the concrete blanket, and the drainage holes in the apron.

(5) Due to the large difference between upstream and downstream water levels in dry season, the seepage gradients in the foundation are larger than those in flood season. As there is no seepage monitoring equipment in those risky regions, visual inspection should be performed, especially in dry season, to monitor whether abnormal seepage phenomenon occurs such as vortices in the reservoir in front of the sluice or large flow with fine soil particles in the drainage hole of the apron. In addition, the length of upstream apron can be extended to increase the seepage path, reduce the seepage gradient, and reduce the risk of seepage damage.

Data Availability

The data used to support the findings of this study are available from the corresponding author upon request.

Conflicts of Interest

The authors declare that they have no conflicts of interest.

Acknowledgments

Financial support provided by the National Key R&D Program of China (no. 2018YFC0407103) is gratefully acknowledged.

References

[1] J. Yan, S. H. Liu, and B. Zhou, "Numerical analysis of the anti-seepage measures for high earth rockfill dam on deep overburden," in *Proceedings of the 2nd International Conference on Civil Engineering, Architecture and Building Materials*, Yantai, China, May, 2012.

[2] V. Nourani and B. F. Nobarian, "Permeability change driving effect on embankment dams case study: the Zonouz embankment dam," in *Proceedings of the 5th IASME/WSEAS International Conference on Water Resources, Hydraulics and Hydrology/4th IASME/WSEAS International Conference on Geology and Seismology*, University of Cambridge, Cambridge, England, February, 2010.

[3] Q. Pan, J. Xu, and D. Dias, "Three-dimensional stability of a slope subjected to seepage forces," *International Journal of Geomechanics*, vol. 17, no. 8, 2017.

[4] W. Dong, "Finite element seepage analysis of the floodwall in South Louisiana," in *Proceedings of the 14th Triennial International Conference on Ports—Gateways to a World of Opportunities*, New Orleans, La, USA, June, 2016.

[5] G. Li, J. Ge, and Y. Jie, "Free surface seepage analysis based on the element-free method," *Mechanics Research Communications*, vol. 30, no. 1, pp. 9–19, 2003.

[6] S. H. Chen, Q. Xu, and J. Hu, "Composite element method for seepage analysis of geotechnical structures with drainage hole array," *Journal of Hydrodynamics*, vol. 16, no. 3, pp. 260–266, 2004.

[7] E. B. Ojo and D. S. Matawal, "Application of artificial neural network in monitoring seepage flow through Dadin Kowa dam, Gombe state Nigeria," in *Proceedings of the 8th European Conference on Numerical Methods in Geotechnical Engineering*, Delft University of Technology, Delft, Netherlands, June, 2014.

[8] T. Jiang, J. Zhang, W. Wan, S. Cui, and D. Deng, "3D transient numerical flow simulation of groundwater bypass seepage at the dam site of Dongzhuang hydro-junction," *Engineering Geology*, vol. 231, pp. 176–189, 2017.

[9] J. Lu, S. Li, W. Li, and L. Tang, "A hybrid inversion method of damped least squares with simulated annealing used for Rayleigh wave dispersion curve inversion," *Earthquake Engineering and Engineering Vibration*, vol. 13, no. 1, pp. 13–21, 2014.

[10] S. Vardakos, M. Gutierrez, and C. Xia, "Back-analysis of tunnel response from field monitoring using simulated annealing," *Rock Mechanics and Rock Engineering*, vol. 49, no. 12, pp. 4833–4852, 2016, in Chinese.

[11] W. Gao, "Inversion of critical slip surface parameters for a landslide disaster using the bionics algorithm," *International Journal of Geomechanics*, vol. 16, no. 5, 2016.

[12] Q. B. Guo, G. L. Guo, X. Lu, T. Chen, and J. T. Wang, "Prediction model for surface subsidence and parameters inversion in valley bottom area," *Rock Mechanics and Rock Engineering*, vol. 37, no. 5, pp. 1351–1356, 2016, in Chinese.

[13] S. P. Jia, J. Gong, M. Gao, J. Z. Luo, and H. D. Yu, "Inversion analysis of permeability coefficients of excavation-disturbed zone around a mudstone roadway with considering self-healing effect," *Rock Mechanics and Rock Engineering*, vol. 36, no. 5, pp. 1444–1454, 2015, in Chinese.

[14] Y. Wu, B. Zhang, Y. Yu, and Z. Zhang, "Consolidation analysis of Nuozhadu high earth-rockfill dam based on the coupling of seepage and stress-deformation physical state," *International Journal of Geomechanics*, vol. 16, no. 3, 2016.

[15] S. Chi, S. Ni, and Z. Liu, "Back analysis of the permeability coefficient of a high core rockfill dam based on a RBF neural network optimized using the PSO algorithm," *Mathematical Problems in Engineering*, vol. 2015, Article ID 124042, 15 pages, 2015.

[16] W. Zhou, S.-L. Li, G. Ma, X.-L. Chang, Y.-G. Cheng, and X. Ma, "Assessment of the crest cracks of the Pubugou rockfill dam based on parameters back analysis," *Geomechanics and Engineering*, vol. 11, no. 4, pp. 571–585, 2016.

[17] S. Zhang, S. Yin, and Y. Yuan, "Estimation of fracture stiffness, in situ stresses, and elastic parameters of naturally fractured geothermal reservoirs," *International Journal of Geomechanics*, vol. 15, no. 1, 2015.

[18] J. Chen, S. Jia, and X. Zhang, "Back analysis and application of confined aquifer hydrogeological parameters based on pumping test," *Geotechnical and Geological Engineering*, vol. 35, no. 6, pp. 2851–2861, 2017.

[19] H. Yang, W. Zhou, G. Ma, S. L. Li, and X. L. Chang, "Inversion of instantaneous and rheological parameters of high rockfill dams based on response surface method," *Rock Mechanics and Rock Engineering*, vol. 37, no. 6, pp. 1697–1705, 2016, in Chinese.

[20] H. Zhao, Z. Ru, and S. Yin, "A practical indirect back analysis approach for geomechanical parameters identification," *Marine Georesources & Geotechnology*, vol. 33, no. 3, pp. 212–221, 2015.

[21] Q. Guo, L. Pei, Z. Zhou, J. Chen, and F. Yao, "Response surface and genetic method of deformation back analysis for high core rockfill dams," *Computers and Geotechnics*, vol. 74, pp. 132–140, 2016.

[22] H. B. Zhao, Z. L. Ru, and C. X. Zhu, "Determination of the geomechanical parameters and associated uncertainties in hydraulic fracturing by hybrid probabilistic inverse analysis," *International Journal of Geomechanics*, vol. 17, no. 12, 2017.

[23] ANSYS, *The Basic Analysis Guide of ANSYS Software*, ANSYS Company, Canonsburg, PA, USA, 2013.
[24] M. Saeed, *Finite Element Analysis: Theory and Applications with ANSYS*, Prentice-Hall, Upper Saddle River, NJ, USA, 2nd edition, 2006.
[25] C. G. Bucher and U. Bourgund, "A fast and efficient response surface approach for structural reliability problems," *Structural Safety*, vol. 7, no. 1, pp. 57–66, 1990.
[26] A. Hadidi, B. F. Azar, and A. Rafiee, "Efficient response surface method for high-dimensional structural reliability analysis," *Structural Safety*, vol. 68, pp. 15–27, 2017.
[27] S. M. Wang, H. W. Zhang, Y. M. Zhang, and J. Zheng, "Back analysis of unsaturated parameters and numerical seepage simulation of the Shuping landslide in Three Gorges reservoir area," in *Proceedings of the 10th International Symposium on Landslides and Engineered Slopes*, Xian, China, June-July 2008.
[28] H. Tian, W. Chen, D. Yang, Y. Dai, and J. Yang, "Application of the orthogonal design method in geotechnical parameter back analysis for underground structures," *Bulletin of Engineering Geology and the Environment*, vol. 75, no. 1, pp. 239–249, 2016.
[29] LINGO, *LINGO 15 User's Guide*, LINDO Systems Inc, Chicago, IL, USA, 2014.
[30] K.-K. Phoon and F. H. Kulhawy, "Characterization of geotechnical variability," *Canadian Geotechnical Journal*, vol. 36, no. 4, pp. 612–624, 1999.
[31] IBM SPSS, *SPSS Base 21.0 Users Guide*, IBM SPSS Statistics, Chicago, IL, USA, 2012.